

SYNTHESIS OF NOVEL MAGNETIC ADSORBENTS FROM COFFEE HUSKS BY HYDROTHERMAL CARBONIZATION

**Tran Thi Hien^{1,*}, Nguyen The Vu², Pham Huu Thien³,
Nguyen Dinh Thanh³, Phan Dinh Tuan⁴**

¹*Industrial University of Hochiminh City, 12 Nguyen Van Bao Str., Go Vap Dist.,
Hochiminh City*

²*Hochiminh City Vocational College of Technology, 502 Do Xuan Hop Str., Dist. 9,
Hochiminh City*

³*Institute of Applied Materials Science-VAST, 1 Mac Dinh Chi Str., Dist. 1, Hochiminh City*

⁴*Hochiminh City University of Natural Resources and Environment,
236B Le Van Sy Street, Tan Binh Dist., Hochiminh City*

*Email: tranhien86@gmail.com

Received: 15 December 2016; Accepted for publication: 3 August 2017

ABSTRACT

Coffee husks were transformed into magnetic adsorption materials by the hydrothermal carbonization (HTC) method at low temperature (180 °C) in the presence of iron (III) salt. For the capability of absorbing methylene blue, the absorbed content by biochar is 105.831 mg/g and by magnetic adsorption material is 263.158 mg/g. Absorption capacity is also described through the isotherm Langmuir model. HTC is demonstrated as an alternative and effective approach in converting waste biomass into materials for waste water treatment.

Keywords: hydrothermal carbonization, magnetic adsorption materials, coffee husks, agricultural waste.

1. INTRODUCTION

Magnetic adsorption is a commonly used method to remove contaminants in water, with its high efficiency and wide adaptability [1, 2]. Most of the adsorbents were recovered by filtration or centrifugation. In recent years, the magnetic adsorbents are of a new research subject in water treatment to attain the adsorbent recovery. Magnetic adsorbents can easily be separated by using an external magnetic field [3, 4]. Currently, the utilization of biomass to make the application of adsorbent in removing contaminants, especially dyes from waste water is a very interesting but challenging task [5, 6]. Coffee husk is a potential source to regenerate new products with high values, environmental protection and sustainable agriculture. However, the regenerative process of coffee husk has some limitations. A fraction of biomass coffee husk is used to produce fertilizer or using as fuels, while the rest is naturally disintegrated. Coffee husks need more time

to be disintegrated than other agricultural wastes, so it's an imperative task to develop new methods for synthesis of magnetic adsorption materials (synthesized within a low temperature condition, non-toxic adsorbents using waste biomasses, or coffee specifically).

Hydrothermal carbonization (HTC) is a promising method for transforming agricultural waste products with high efficiency [7]. It has the capability of decomposing biomass feedstock sources with high humidity (up to 80 %) at low temperature of about 160 – 270 °C, for different carbon materials. HTC reactions beproceed with the same level of conversion efficiency as higher temperature processes [8]. Therefore, the development of HTC at low temperature for transforming coffee husks into magnetic adsorption materials is essential. The objective of this study was to use HTC to metabolize coffee husk to produce carbonaceous material precursor and magnetic carbonaceous adsorbents for removal of methylene blue. Adsorption of two types of materials is described through the Langmuir adsorption isotherm and the Freundlich model [9].

2. EXPERIMENTAL

2.1. Materials

Coffee's husk was collected from grinding factory located in Buon Ma Thuot city, Daklak, Vietnam (Robusta coffee, *Coffea Canephora*). Before being dried, coffee husks were milled into powder and collected through a 250-mesh sieve.

2.2. Preparation of the adsorption materials

2.2.1. Biochar (B)

Biochar (B) was prepared via hydrothermal carbonization of coffee husk using distilled water. The coffee husk to water ratio of 15 % was maintained in a 400 mL sealed, teflon-lined autoclave at 180 °C for 3.5 hours. After cooling to room temperature, biochar was collected by vacuum filtration, washed with deionized water and dried at 105 °C. The yield of the final biochar obtained was 59.7 %.

2.2.2. Magnetic adsorption materials (MAM)

The magnetic coffee-derived adsorbent, a kind of MAM, was synthesized by magnetization of the carbonized coffee husks in a solution. Briefly, the mixture of biochar and $\text{FeCl}_3 \cdot 6\text{H}_2\text{O}$ with 2:1 ratio was dispersed in 2.5 M NaOH solution with continuous stirring for 0.5 hour to obtain a homogeneous dispersion. The resulting mixture was then placed into a 400 mL sealed, teflon-lined autoclave and maintained at 180 °C for 8 hours. After cooling to room temperature, the magnetic coffee-derived adsorbent was collected by a laboratory magnet, washed with deionized water until $\text{pH} = 7$ and dried at 80 °C for 7 hours. In such a hydrothermal magnetization, the yield of the final MAM obtained was 65 %, which was calculated based on the initial amount of B.

2.3. Material characterizations

The microstructures of the magnetic adsorbents were analyzed by X- ray diffraction (XRD). The XRD analysis was performed using Siemens D-5000, with a sweep angle of 10-70 degree, a scan step of 0.03 degree and a scan speed of 0.7 degree/second. Surface and structural

features were analyzed by scanning electron microscopy (SEM) and transmission electron microscopy (TEM) images. SEM was calculated by SEM – Hitachi S 4800 device, while TEM was taken by JEOL JEM – 1400. Specific surface areas were measured using a nitrogen adsorbed method, while their pore volumes were calculated by the amount of nitrogen adsorption–desorption isotherm performing at temperature 77 K through Quantachrome NOVA 1000e. The magnetization curves of MAM were recorded using EV11 vibrating sample magnetometer (EV11 VSM, USA) at HCMIP- VAST .

2.4. Methylene blue adsorption experiments

The concentration of the adsorbent in the adsorption isotherm testing was 1 g/L, and the MB concentration changed from 50 to 500 mg/L with the increasing gradient of 50 mg/L. These experiments were carried out at 25 °C, and all suspensions were shaken on the rotary shaker Jarrest at a speed of 100 rpm for 16 hours to reach an adsorption equilibrium.

3. RESULTS AND DISCUSSION

3.1. Characterizations of B and MAM

The surface area of MAM was measured to be 142.32 m²/g, significantly higher than that of B as 48.84 m²/g. This result corresponds well to other studies of magnetic carbon-based adsorbents, such as: MCA (153.89 m²/g) [8], MWCNT-iron oxide (124.86 m²/g) and MWCNT-starch-iron oxide (132.59 m²/g) [10]. This result revealed that the presence of Fe species when the magnetization of B under hydrothermal condition, e.g., ferrous compounds (FeO(OH), Fe₂O₃ or Fe₃O₄) as an agent to create porous structure, leading to the increase in surface area and the increased adsorption capacity. This is in agreement with the results reported by Liu et al. [11]. The small nano-ferrous compounds not only facilitated the separation of adsorbent, but may also lead to a relatively rough surface and even form a porous structure in the framework of MAM. All of these would result in the increase of the surface area, which could improve the adsorption efficiency.

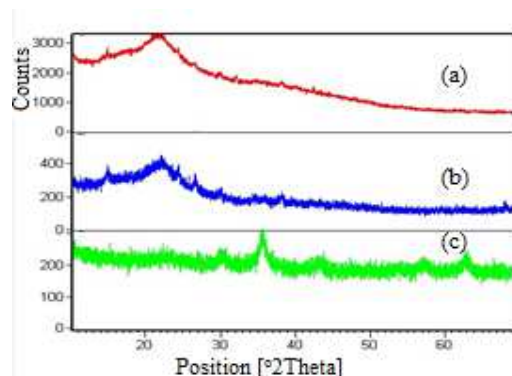


Figure 1. XRD patterns of a coffee husk (a), a biochar (b) and a magnetic adsorption material (c)

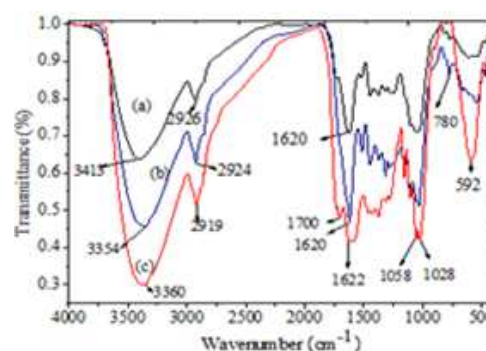


Figure 2. FTIR spectra of coffee husk (a), biochar (b) and magnetic adsorption material (c)

As shown in Fig. 1 the XRD patterns in comparison to the raw coffee husk, the characteristic peaks of lignocellulose became more obvious in B, showing that a single hydrothermal process only removed impurities without destroying the “core” structure of coffee husks. However, after the hydrothermal carbonization, signals of lignocellulose were completely

depleted, the XRD pattern for B, a broad diffraction peak ($2\theta = 15 - 30^\circ$). These results were in agreement with the work of Liu et al. [11] and suggested the formation of phase Fe_3O_4 by appearance of diffraction peaks at 2θ of about $30.1, 35.6, 37.1, 43.1, 53.4, 56.9$ and 62.5° .

Figure 2 shows the results of Fourier transform infrared spectroscopy (FTIR) in comparison to the raw coffee husk, the characteristic vibration peaks of functional groups ($-\text{OH}$: 3354 cm^{-1} , C-H : 2924 cm^{-1} , C=C : 1620 cm^{-1}) of lignocellulose became more obvious in B. After the hydrothermal carbonization process, the vibration was enhanced and obvious in the structure.

It should be noted that the peak 1700 cm^{-1} was enhanced after the hydrothermal treatment, indicating the surface of MAM was modified by more oxygen-containing functional groups. As suggested in a previous study by Huan et al. [12]. Compared to B, the most obvious change in MAM was the appearance of peak about 592 cm^{-1} after magnetization, which was identified as the characteristic absorption peak of Fe_3O_4 [14]. The combination of the oxygen-containing functional groups into adsorbents may play an important role in the dye adsorption by means of specific adsorption such as H-bonding and $\pi - \pi$ interaction. Moreover, the higher content of $-\text{OH}$ group may result in an enhanced absorption capacity of the magnetic carbonaceous adsorbent, improving hydrophilic property, dispersion performance ability [14].

Figure 3 shows the typical SEM images of B and MAM that were formed in a porous and stratiform structure, unequal in particle sizes. To be more specific, MAM particle size varies from 238 nm to $1.18\text{ }\mu\text{m}$ and B is larger ranging from 472 nm to 609 nm . The SEM results were also verified by the results of the sample BET biochar and magnetic adsorption material at $48.84\text{ m}^2/\text{g}$ and $142.32\text{ m}^2/\text{g}$, respectively. This leads to a general expectation that the adsorption ability of MAM will be better than that of B.

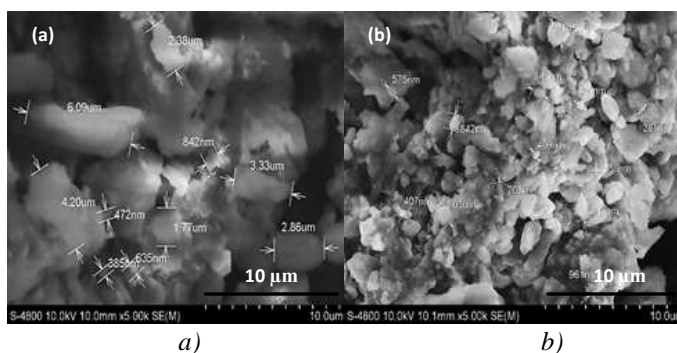


Figure 3. SEM images of biochar (a) and magnetic adsorption material (b).

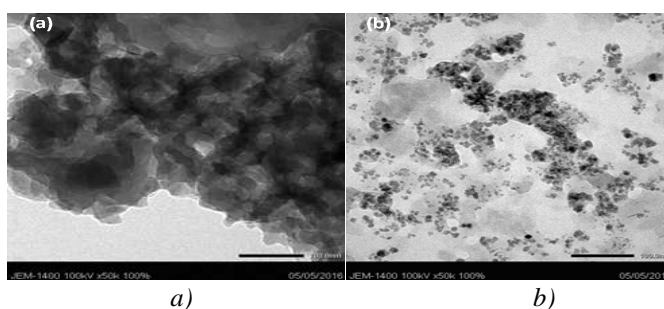


Figure 4. TEM images of the biochar (a) and the magnetic adsorption material (b).

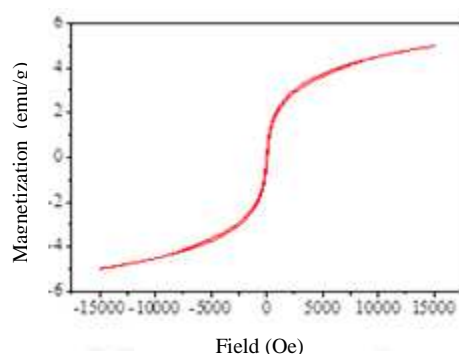


Figure 5. Magnetic curves of BTT.

Figure 4 indicates that both materials don't have specific shapes; but they are parts, layers overlap each other. It is obvious from Fig. 4b that dark nano-particles ferrous compounds attached to the MAM molecules are responsible for the high adsorption performance. These particles also help separate MAM by using an external magnetic field. The magnetic ferrous compounds nanoparticles were considered to be successfully installed on the carbonaceous precursor, which was supported with the XRD and FTIR results. Moreover, all of these results revealed that the two materials possessed a porous structure, which is favorable for the rapid diffusion of dye by providing interconnected and low-resistance channels for the dye.

Magnetic measurement was performed on MAM using a vibrating sample magnetometer, and the result of which is shown in Fig. 5. From the M-H loop, we have determined the maximum magnetization ($M_{\max} = 4.983 \text{ emu/g}$), the remanent magnetization ($M_r = 158.802 \times 10^{-3} \text{ emu/g}$), and the coercivity ($H_c = 26.34 \text{ Oe}$). This indicates that there is a significant amount of ferrous compounds joining the network in line with the results of SEM, TEM and appearance of the 592 cm^{-1} peak in the FTIR spectrum, confirming the material surcharges MAM and can thus be separated by the magnet.

3.2. Adsorption isotherm equilibrium

Adsorption isotherm is a line describing the dependencies between adsorption capacity at equilibrium concentration on the adsorbent in the solution at that time, and are also critical for optimization of the adsorption system [9]. The adsorption isotherms of MB onto B and MAM were shown in Fig.6a at low C_e values (the equilibrium concentration in the solution), the adsorption capacity (q_e) of both B and MAM increased quickly. But once C_e was greater than 150 mg/L for B and 100 mg/L for MAM the adsorption capacity (q_e) increased slowly. The maximum adsorption capacities of MB were 105.83 mg/g for B and 263.16 mg/g for MAM, respectively. It should be noted that MAM obtained in our work exhibited more competitive adsorption ability for MB than other magnetic carbon-based adsorbents, such as MCA (163.93 mg/g) [8], MWCNT-iron oxide (52.7mg/g) and MWCNT-starch-iron oxide (94.1 mg/g) [10], magnetic hydrotalcite (110.05 mg/g) [15] and magnetic grapheme nanosheet (43.82 mg/g) [16]. Lots of isotherm equations can be utilized to establish the correlation, such as Langmuir, Freundlich models [9].

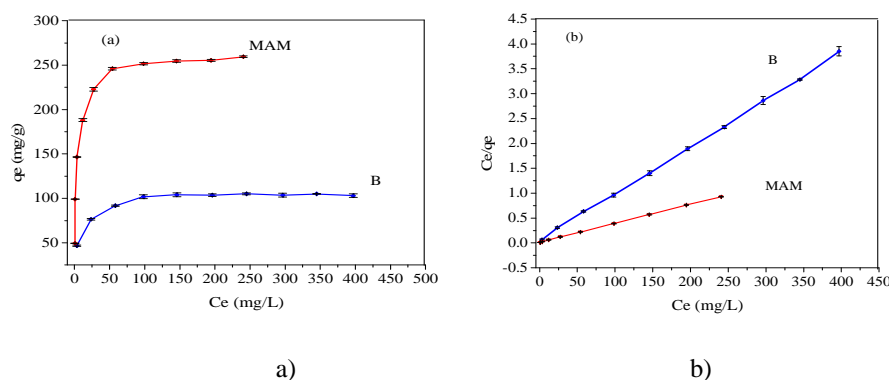


Figure 6. Adsorption isotherms for MB on B and MAM (a), the Langmuir isotherm plots for adsorption of MB on B and MAM (b).

Table 1. Isotherms parameters of MB adsorption on B and MAM.

Isotherms model	Parameters	B	MAM
Langmuir	Q_m (mg/g)	105.831	263.158
	K_L (L/mg)	0.18757	0.30645
	R_L	0.01055 - 0.09635	0.00648 - 0.06126
	R^2	0.9995	0.9998
Freundlich	K_F ((mg/g)(L/mg) ^{1/n})	43.19791	89.2195
	n	6.13497	4.43262
	R^2	0.8998	0.8534
Q_{exp}	Q_{exp} (mg/g)	105.1453 ± 0.97804	259.438 ± 1.00751

The adsorption isotherm constants of B and MAM were listed in Table 1. The relatively low value (< 0.9) of the liner correlation coefficient R^2 indicated that the unsuitability of Freundlich isotherm models for B and MAM. The values of R^2 for Langmuir model (0.9995 for B and 0.9998 for MAM) were high, indicating that this model can be used to characterize the equilibrium adsorption. In addition, according to the Langmuir model, the calculated maximum MB uptake of B and MAM were quite close to their corresponding experimental data (Q_{exp}) (Table 1).

As shown in Fig. 6b, the experimental data fitted the theoretic Langmuir simulated curves fairly well, indicating the monolayer adsorption for MB on B and MAM [17]. Furthermore, the results indicated that the adsorption of MB onto B and MAM was a dynamic chemisorption process by the adsorption affinity in terms of surface functional groups and bonding energy [9, 18]. The maximum adsorption capacity (Q_m) for MB on B and MAM were 105.83 mg/g and 263.16 mg/g, respectively, which were determined from the linear plot of C_e/q_e versus C_e of the Langmuir model and very close to the experiment data. Furthermore, a dimensionless constant called separation factor (R_L) was applied to evaluate the suitability of an adsorption process. The R_L can be calculated from the constant K_L [9, 19]:

$$R_L = \frac{1}{1 + K_L C_o}$$

where C_0 (mg/L) is the initial dye concentration in solution and K_L (L/mg) is the Langmuir isotherm coefficients related to the free energy of adsorption.

The value of R_L describes the tendency of the adsorption process, which is either unfavorable ($R_L > 1$), linear ($R_L = 1$), favorable ($0 < R_L < 1$), or irreversible ($R_L = 0$). Greater affinity between the adsorbent and the adsorbate is inferred when R_L is smaller. The R_L values were in the range of 0.01055 – 0.09635 for B and 0.00648 – 0.06126 for MAM, favorable ($0 < R_L < 1$), which implies that the adsorption of MB onto both B and MAM was a favorable and useful process. Moreover, the R_L value for MAM was smaller than that for B, thus it can be concluded that the adsorption capacity for MB of MAM is enhanced by the increase of the surface area of B after the process of magnetization, consistent with the results observed during the adsorption.

4. CONCLUSIONS

A novel magnetic adsorbent derived from coffee husk was successfully synthesized by the HTC method in the presence of iron (III) salt and low temperature conditions (180 °C). The resulting MAM enhanced the adsorption capacity for different dyes, due to its porous structure, high surface area and large amounts of active adsorption sites resulting from the catalytic effect of ion Fe (III) salt. The adsorption behaviors of both B and MAM could be described well by the Langmuir isotherm model B and MAM still retained the satisfactory adsorption capacity for MB even after six and seven cycles of reuse respectively (adsorption performance more than 50 %).

Acknowledgements. The Institute of Applied Materials Science and the Industrial University of Hochiminh City were highly appreciated for financial support to this study.

REFERENCES

1. Huang Y. and Keller A. A. - Magnetic Nanoparticle Adsorbents for Emerging Organic Contaminants, *ACS Sustainable Chemistry & Engineering* **1** (7) (2013) 731-736.
2. Mohan D., Sarswat A., Ok Y. S., and Pittman Jr C. U. - Organic and inorganic contaminants removal from water with biochar, a renewable, low cost and sustainable adsorbent – A critical review, *Bioresource Technology* **160** (2014) 191-202.
3. Devi P. and Saroha A. K. - Synthesis of the magnetic biochar composites for use as an adsorbent for the removal of pentachlorophenol from the effluent, *Bioresource Technology* **169** (2014) 525-531.
4. Lu W., Shen Y., Xie A., and Zhang W. - Preparation and Protein Immobilization of Magnetic Dialdehyde Starch Nanoparticles, *The Journal of Physical Chemistry B* **117** (14) (2013) 3720-3725.
5. Liu R. L., Liu Y., Zhou X. Y. - Biomass-derived highly porous functional carbon fabricated by using a free-standing template for efficient removal of methylene blue, *Bioresource Technology* **154** (2014) 138-147.
6. Zhu X., Liu Y., Zhou C., Zhang S., and Chen J. - Novel and High-Performance Magnetic Carbon Composite Prepared from Waste Hydrochar for Dye Removal, *ACS Sustainable Chemistry & Engineering* **2** (4) (2014) 969-977.

7. Oliveira I., Blöhse D., and Ramke H. G. - Hydrothermal carbonization of agricultural residues, *Bioresource Technology* **142** (2013) 138-146.
8. Ma H., Li J. B., Liu W. W. - Novel synthesis of a versatile magnetic adsorbent derived from corncob for dye removal, *Bioresource Technology* **190** (2015) 13-20.
9. Cao J. S., Lin J. X., Fang F., Zhang M. T., and Hu Z. R. - A new adsorbent by modifying walnut shell for the removal of anionic dye: Kinetic and thermodynamic studies, *Bioresource Technology* **163** (2014) 199-205.
10. Yan L., Chang P. R., Zheng P., and Ma X. - Characterization of magnetic guar gum-grafted carbon nanotubes and the adsorption of the dyes, *Carbohydrate polymers* **87** (3) (2012) 1919-1924.
11. Liu W.J., Tian K., He Y.R., Jiang H., Yu H.Q. - High-yield harvest of nanofibers/mesoporous carbon composite by pyrolysis of waste biomass and its application for high durability electrochemical energy storage, *Environmental Science & Technology* **48** (23) (2014) 13951-13959.
12. Ma H., Li J., Liu W. - Hydrothermal Preparation and Characterization of Novel Corncob-Derived Solid Acid Catalysts, *Journal of Agricultural and Food Chemistry* **62** (23) (2014), 5345-5353.
13. Chang P. R., Zheng P., Liu B. - Characterization of magnetic soluble starch-functionalized carbon nanotubes and its application for the adsorption of the dyes, *Journal of Hazardous Materials* **186** (2-3) (2011) 2144-2150.
14. Geng Z., Lin Y., Yu X. - Highly efficient dye adsorption and removal: a functional hybrid of reduced graphene oxide-Fe₃O₄ nanoparticles as an easily regenerative adsorbent, *Journal of Materials Chemistry* **22** (8) (2012) 3527-3535.
15. Miranda L. D. L., Bellato C. R., Fontes M. P. F. - Preparation and evaluation of hydrotalcite-iron oxide magnetic organocomposite intercalated with surfactants for cationic methylene blue dye removal, *Chemical Engineering Journal* **254** (2014) 88-97.
16. Ai L., Zhang C., and Chen Z. - Removal of methylene blue from aqueous solution by a solvothermal-synthesized graphene/magnetite composite, *Journal of Hazardous Materials* **192** (3) (2011) 1515-1524.
17. Yang X., Wang Z., Jing M. - Efficient removal of dyes from aqueous solution by mesoporous nanocomposite Al₂O₃/Ni_{0.5}Zn_{0.5}Fe₂O₄ microfibers, *Water, Air, & Soil Pollution* **225** (1) (2014) 1-12.
18. Dawood S. and Sen T. K. - Removal of anionic dye Congo red from aqueous solution by raw pine and acid-treated pine cone powder as adsorbent: Equilibrium, thermodynamic, kinetics, mechanism and process design, *Water Research* **46** (6) (2012) 1933-1946.
19. Zhou Y., Fu S., Zhang L., Zhan H., and Levit M. V. - Use of carboxylated cellulose nanofibrils-filled magnetic chitosan hydrogel beads as adsorbents for Pb(II), *Carbohydrate Polymers* **101** (2014b) 75-82.